

PROGRESS AND TRENDS IN AIR INFILTRATION AND VENTILATION RESEARCH

10th AIVC Conference, Dipoli, Finland
25-28 September 1989.

Poster 12

BUOYANCY-DRIVEN AIR FLOW IN A CLOSED HALF-SCALE STAIRWELL
MODEL: VELOCITY AND TEMPERATURE MEASUREMENTS

A.S. ZOHRABIAN, BSc, MSc - PhD Research Student

M.R. MOKHTARZADEH-DEHGHAN, BSc, MSc, DIC, PhD, MASME, AMIMEchE -
Lecturer,

A.J. REYNOLDS, BSc, PhD, DIC, CEng, FIMEchE, MASCE, FRSA -
Professor and Head of Department of Mechanical Engineering.

Department of Mechanical Engineering, Brunel University, Uxbridge,
Middlesex, UB8 3PH, England.

SUMMARY

This paper describes an experimental study of the buoyancy-driven flow and the associated energy transfer within a closed, half-scale stairwell model. It provides new data on the velocity, temperature, volume and mass flow rates of the air circulating between the upper and lower storeys. The results are presented for various heat input rates from the heater, located in the lower floor. For most of the data presented, heat transfer to the surrounding atmosphere takes place through the side walls. However, the case of insulated side walls is also included and the effects on the parameters of interest are discussed. The velocities were measured using hot-wire anemometers of a temperature compensated type, and the temperatures were measured using platinum resistance thermometers. These measurements were supported by flow visualisation using smoke. The paper also provides data on the rate of leakage through the stairwell joints, measured using a concentration decay method.

LIST OF SYMBOLS

A	Throat area (0.462 m^2)
C, c	Concentration inside and outside stairwell (ppm).
c_p	Specific heat at constant pressure ($\text{J kg}^{-1} \text{ K}^{-1}$).
DT	Differential temperature ($T_H - T_C$), (C deg.).
g	Gravitational acceleration (m s^{-2}).
h	One half the height of the stairwell model (m).
k	Heat conductivity ($\text{J m}^{-1} \text{ s}^{-1} \text{ K}^{-1}$).
\dot{m}_u, \dot{m}_d	Upflow and downflow mass flow rates (kg s^{-1}).
\dot{m}_l	Leakage rate (kg s^{-1}).
\dot{Q}	Rate of supply of heat to the stairwell (W).
\dot{Q}_s	Volume flow rate through leakage ($\text{m}^3 \text{ s}^{-1}$).
T_{av}	Average temperature within the stairwell ($^{\circ}\text{C}$).
T_H, T_C	Mean temperatures of warm upwards-flowing air and cold downwards-flowing air, respectively ($^{\circ}\text{C}$).
U_{maxu}	Maximum velocity of the flow moving up the stairwell (m s^{-1}).
U_{maxd}	Maximum velocity of the flow moving down the stairwell (m s^{-1}).
V_s	Stairwell volume (m^3).
\dot{V}_m	Arithmetic average of the volume flow rates, of the upflow and downflow ($\text{m}^3 \text{ s}^{-1}$), $\dot{V}_m = (\dot{V}_u + \dot{V}_d)/2$.
\dot{V}_u, \dot{V}_d	Upflow and downflow volume flow rates ($\text{m}^3 \text{ s}^{-1}$).
w	Stairwell width (m).
z	Direction along the throat area (see Figure 1).

GREEK SYMBOLS

β	Coefficient of thermal expansion (K^{-1})
ρ	Fluid density (kg m^{-3})
ν	Kinematic viscosity ($\text{m}^2 \text{ s}^{-1}$)
μ	Dynamic viscosity ($\text{kg m}^{-1} \text{ s}^{-1}$)

DIMENSIONLESS GROUPS

Fr	Froude number	=	$\frac{\dot{V}_m}{A (gh)^{1/2}}$
Gr	Grashof number	=	$\frac{g \beta DT Ah}{\nu^2}$
Pr	Prandtl number	=	$\frac{\mu C_p}{k}$
Ra	Rayleigh number	=	Gr.Pr
Re	Reynolds number	=	$\frac{\dot{V}_m}{\nu A^{1/2}}$
St	Stanton number	=	$\frac{\dot{Q}}{\rho C_p T_{av} A (gA)^{1/2}}$

DEFINITIONS

Throat area : The area shown by DD' in Figure 1.

Side wall : Area defined by ACDEFDHIA in Figure 1.

1. INTRODUCTION

Obtaining a better understanding of the mechanism and characteristics of air movement within stairwells, in private dwellings, hotels and public buildings such as hospitals and underground stations, is important in relation to wide ranging problems such as fire safety, energy saving and movement of micro-organisms and contaminants. Improvements in the basic understanding can be obtained by carrying out simple tests on small-scale models, setting up simple analytical models or using high-level computational models.

Fires account annually for thousands of deaths and millions of pounds in loss of property. Moodie et al.⁽¹⁾ have carried out experiments on a one-third scale model of an escalator to investigate the fire which occurred in King's Cross underground station in 1987. The results showed that, following the ignition, the flame was soon established across the full width of the escalator channel. The flame front then remained low in the escalator channel as the fire developed and then progressed in the escalator. Zohrabian et al.⁽²⁾ have shown that sloping the stairwell ceiling speeds up the migration of smoke from the lower to the upper compartment, hence helps in the spread of fire.

Most rooms in hospitals are connected by corridors and stairwells. The importance of movements of micro-organisms in a hospital stairshaft has been shown by several workers in recent years. The measurements by Münch et al.⁽³⁾ indicate that transport of micro-organisms depends on the temperature differential within the stairwell. The experimental measurements of Zohrabian et al.⁽²⁾ on a half-scale stairwell model showed that the volume flow rate of the air flow from the lower floor to the upper was increased by increasing the heating load or changing the stairwell geometry. Hence micro-organisms, as well as toxic agents or contaminants which can cause wound infection, can be transferred to the upper floors by way of the stairwell. Therefore, special arrangements or appropriate stairwell design is needed within hospital buildings, in order to minimize the flow of unwanted germs or contaminants to the higher floors.

A number of other useful experimental studies are reported by Brown and Solvason⁽⁴⁾, Shaw⁽⁵⁾, Shaw and Whyte⁽⁶⁾, Feustel et al.⁽⁷⁾, Marshall^(8,9), Mahajan⁽¹⁰⁾, Riffat et al.⁽¹¹⁾ and Riffat and Eid⁽¹²⁾. Analytical modelling of relevant flows are reported by Reynolds and Reynolds et al.^(13,14), Nevrala and Probert⁽¹⁵⁾, Liddament⁽¹⁶⁾. Applications of Computational Fluid Dynamics to flows relevant to buildings have increased in recent years. But, to the best of the present authors' knowledge, the only applications to stairwell flows have been by Zohrabian et al.⁽¹⁷⁾ and Simcox and Schomberg⁽¹⁸⁾. The latter authors used HARWELL-FLOW3D code to investigate the King's Cross fire.

The present work extends the previous study by Zohrabian et al.⁽²⁾ by providing new data on the characteristics of buoyancy-driven flows in a half-scale stairwell model.

2. EXPERIMENTAL RIG AND INSTRUMENTATION

A schematic diagram of the half-scale stairwell model is shown in Figure 1. The details of instrumentation can be found in Ref. [2]. Therefore, only a brief reference to the instrumentation and the improvements of the original model is made here.

The velocities were measured using hot wires of temperature compensated type having a time constant of about 1s and accuracy of less than 10 per cent for the range of velocities measured within the stairwell. The temperatures were measured using platinum resistance thermometers having a time constant of 3 min and accuracy of $\pm 0.25^{\circ}\text{C}$. The probes were fixed to the walls by specially designed clamps. The signals from these probes were transferred to an Apple computer for processing, via signal conditioning electronics and Analogue-to-Digital converters.

The modifications to the rig described in reference [2] were:

- (i) The light bulbs used as heat source were replaced by an electric radiator with surface area of $0.57 \text{ m} \times 0.659 \text{ m}$ and with a loading power of 1 kW.
- (ii) Both side walls were made of Perspex of 10 mm thickness (originally one of the walls was made of Perspex of 12.5 mm thickness and the other made of wood of 18 mm thickness). This ensured better thermal symmetry in the stairwell.

3. RESULTS

3.1. Flow characteristics

A two-dimensional view of the flow pattern is shown in Figure 2. The main recirculating flow, recirculation zones, and upward and downward flows in the stairway can be seen. Comparison with previous work [2] showed that, although some changes had been introduced into the design of the rig and completely different type of heat source was used (see section 2), the overall characteristics of the flow did not change significantly. For further detail see reference [2].

3.2. Velocity and temperature profiles in the throat area

Figures 3 and 4 show, respectively, the velocity and temperature distributions at various distances from the side wall and for various heat input rates. The results indicate two distinct regions: one associated with the warm upflow, in the upper part of the throat area, and one with the cold downflow, in the lower part. The results indicate an increase in velocity to a maximum very close to the ceiling, after which it drops to zero at the ceiling. The maximum velocity varies from about 0.24 m/s at 100 W to about 0.54 m/s at 900 W heat input rate. Figure 4 shows that the temperature varies approximately linearly from its lowest value near the stairs to a maximum very near to the ceiling of the throat area. The same behaviour can be seen for other heat input rates. As expected, the increase in heat input rate has resulted in an increase in velocity and temperature of the recirculating flow. The temperature data also show that the maximum temperature varies from approximately 31°C at 100 W to about 56° at 900 W heat

input rate.

In order to obtain some idea of the three-dimensional behaviour of the flow, the above results are also presented in an alternative way. Figures 5 and 6 show, respectively, the velocity and temperature profiles at various distances from the side wall. Figure 5 shows that the velocity profiles can be considered uniform over about two-thirds of the width of the stairwell. Therefore, the overall fluid flow may be considered as two-dimensional. Figure 6 shows higher temperatures for higher heat input rates. Also, the temperature profiles show higher degree of uniformity, across the stairwell, for higher input rates. This uniformity is even more pronounced in the upper region of the throat area. However, it is interesting to note that, although, as expected, the lowest temperatures were measured at position $w/6$, the highest temperatures were not recorded at the mid-width of the stairwell (except for the 100 W heat input rate), but at $w/3$. This indicates complex flow behaviour near the stairs.

3.3. Leakage Measurement

Figure 7 shows the results of the tracer-decay test for a 100 W heat input rate. It shows variations of CO_2 tracer gas concentration against time. The negative slope of the line is equal to the air change rate, given by

$$\dot{Q}_s/V_s = \text{Air change rate}$$

where V_s is the stairwell volume, and \dot{Q}_s is the volume flow rate through leakage.

However, for the actual volumetric air flow rate, or air leakage rate in this case, the stairwell volume was multiplied by the air change rate. Table 1 gives the air leakage rates through the stairwell joints, for various heat input rates. The results indicate that the leakage rate increases with heat input rate. It should be noted that the calculation of leakage mass flow rate was based on the arithmetic average T_{av} and room temperature. The calculation of leakage heat flow rate was based on the difference between T_{av} and the room temperature.

3.4. Maximum velocities, mean temperatures and flow rates

Table 2 shows the maximum velocities and mean temperatures in the upflow and downflow streams at various distances from the side wall and for various heat input rates. The results indicate that the maximum air velocity varies slightly across the width of the throat area. It should be noted that calculations of the mean temperatures were based on the arithmetic mean of the temperatures measured in the warm upflow and cold downflow.

Table 3 shows the volume and mass flow rates for various heat input rates. The results show that the volume and mass flow rates increase as the heat input rate increases. The variation of the average volume flow rate \dot{V}_m , with the heat input rate \dot{Q} , can be written in the following form, as suggested by Reynolds⁽¹³⁾.

$$\dot{V}_m \propto \dot{Q}^n$$

It was found that $n=0.22$. This is in agreement with the previous results [2] and also is generally consistent with the model described by Reynolds⁽¹³⁾, in which the value of 0.25 was suggested.

Assuming that the inflow and the outflow through cracks take place in the lower and upper compartment, respectively, one expects that $\dot{m}_u = \dot{m}_d + \dot{m}_l$. The results of table 3 show that the two sides of above relationship differ by less than 5 per cent. The possible reasons for this discrepancy are given in section 4.3.

3.5. Rate of heat loss through the stairwell

Table 4 gives the rate of heat loss from the stairwell for various heat input rates. The results show that the heat losses through the several stairwell boundaries vary approximately linearly with the heat input rate. The results also indicate that over 50 per cent of the heat is lost through the stairwell side walls (for further discussion see section 4.4).

3.6. Effect of insulated side walls on the results

Table 5 shows the rate of heat loss from the stairwell with insulated side walls. The results show a substantial increase in the rate of heat transfer through the other walls. For example, the rate of heat transfer through the upper compartment ceiling has tripled. The results (not given here) also showed that higher velocities and temperatures resulted, both in the upflow and in the downflow streams.

4. DISCUSSION

4.1. Characteristic dimensionless numbers

The characteristic dimensionless numbers relevant to the natural convection in stairwell flows are Froude, Stanton, Reynolds and Grashof numbers. Table 6 gives values of the dimensionless numbers for the half-scale stairwell geometry. Full discussion of their range for the half-scale model is given by Reynolds et al.⁽¹⁴⁾. The corresponding values for full-scale stairwells can be found using the scaling principles set out by Reynolds⁽¹³⁾. These are based effectively on Froude scaling. For example, for a Froude number about 1.4 times the prototype value, requires that the ratio of the energy input of the model to the prototype be 0.24. With this Froude scaling, the magnitudes of the temperatures and velocities become identical in full and model scales. Using this scaling for various heat input rates, the dimensionless numbers at the throat area were in the ranges :

$$0.01385 < Fr < 0.0313 \quad , \quad 0.1765 \times 10^{-3} < St < 1.5845 \times 10^{-3}$$

$$2060 < Re < 4400 \quad , \quad 9.7330 \times 10^7 < Gr < 3.8190 \times 10^8$$

on the half scale and

$$0.0089 < Fr < 0.0224 , \quad 0.130 \times 10^{-3} < St < 1.1668 \times 10^{-3}$$
$$4160 < Re < 8900 , \quad 8.024 \times 10^8 < Gr < 3.1480 \times 10^9$$

on the equivalent full scale.

It should be noted that :

- (i) The fluid properties were evaluated at the arithmetic mean of the 45 temperature readings distributed within the upper and lower compartments.
- (ii) The volume flow rates used for the calculation of Reynolds and Froude numbers were based on the average of the up-flow and downflow volume flow rates.

The flow characteristics in the lower compartment may be understood by reference to the Rayleigh number. One of the most common, and simplest natural convection problems occurs when a vertical heated flat plate transfers heat to a still, colder surrounding fluid. This is approximately the case close to the heater, where, depending upon fluid properties and the thermal gradient, transition to turbulent flow occurs when Rayleigh number is about 10^9 . The Rayleigh number, based on the heater height, the difference between the surface temperature of the heater and that of the surrounding fluid, and the fluid properties evaluated at the arithmetic mean of the temperatures measured in the lower compartment, was found to be within the range 4.361×10^8 to 1.763×10^9 , for 100 W to 900 W heat input rates, respectively.

4.2. The velocity and temperature distributions in the throat area

The flow was symmetrical with respect to the mid-plane of the stairwell. This was examined by measuring temperatures and velocities at the throat area at $w/2$, $w/3$ and $w/6$ distances from both side walls of the stairwell. There was a discrepancy of less than 2 per cent between the temperatures and less than 3 per cent between the velocities measured from the two sides. Therefore, a symmetrical condition was assumed with respect to the mid-plane of the throat area, and the measurements were carried out in only one half of the stairwell.

4.3. Volume and mass flow rates and factors affecting their accuracy

Table 3 gives the flow rates in the upflow and downflow at the throat area for various heat input rates. As mentioned in section 3.4, the results indicate a discrepancy of less than 5 per cent between the upflow and downflow (including leakage) rates. This discrepancy can be attributed mainly to experimental errors and the calculation procedure using Simpson's rule. Moreover, the zero velocity did not usually coincide with the mid-height of the throat area. However, this was assumed for the calculation of volume flow rates, as determination of the actual position, which varied with time, was difficult. Finally, the nearest point at which the velocity could be measured was 10 mm from the wall. Therefore, for locations closer to the wall the velocities were measured using a less accurate air velocity meter.

4.4. Heat transfer rates through the stairwell walls and joints

The heat transfer rates through the stairwell are given in Table 4. The results indicate that more than half of the heat input to the stairwell is lost through the side walls. The results also indicate that there is a difference of less than 3 per cent between the measured heat input rate to the stairwell and the rate of measured heat loss from the stairwell. This error in the heat balance can be attributed to the following facts :

- (i) The calculation of the heat loss was based on the surface temperatures measured at the mid-plane of the stairwell, and were assumed uniform across its width. However, limited measurements showed that for a heat input of 600 W, the surface temperature varied by 0.4C deg.
- (ii) The heat input rate to the radiator was determined from recordings of voltage and current. The accuracy of the heat input rate was about 2 per cent.

In order to investigate the effect of the heat transfer rate through the side walls on the velocity and temperature profiles at the throat area, the side walls of the stairwell were insulated. Table 5 gives the heat transfer rates for this case. The results (not shown here) indicated that insulation of the side walls resulted in an increase in temperatures in the throat area of approximately 3C deg. for 300 W and between 5C deg. to 8C deg. for 600 W heat input rates, respectively. Also, the velocities at the throat area increased by up to 13 per cent in the upflow and up to 15 per cent in the downflow, for 300 W and 600 W heat input rates, respectively. The results also indicated that insulation of the side walls resulted in a significant increase in the rate of heat transfer through the other walls. For example, the rate of heat transfer through the upper-compartment ceiling increased by about 60 per cent for both 300 W and 600 W heat input rates. Furthermore, the Reynolds number increased by 20 per cent, and the Grashof number by about 6 per cent.

5. CONCLUDING REMARKS

This paper has addressed a number of questions left open in the authors' earlier studies of stairwell flows. The symmetry of the flow, and influences which give rise to departures from it, have been investigated. Tracer-gas determinations of the leakage rate from the nominally sealed test rig have been carried out, and the results have been used to analyse discrepancies in other measurements. The influence of thermal boundary conditions has been studied, and the distribution of heat outflows through the boundaries of the stairwell system has been clarified.

Taken together, these additional measurements provide a more comprehensive and convincing picture of the processes involved in this family of buoyancy-driven flows.

ACKNOWLEDGEMENTS

The authors would like to acknowledge the helpful information which they received from the Air Infiltration and Ventilation Centre (AIVC), and Fire Research Station (FRS). They also wish to thank the Science and Engineering Research Council for financial support given as part of the 'Energy in Buildings' Specially Promoted Programme.

REFERENCES

1. MOODIE, K., JAGGER, S.F., BETTIS, R.J. and BECKETT, H.
"Fire at King's Cross Underground Station - Scale model fire growth tests".
Health and Safety Executive, Research and Lab. Services.
Harpur Hill, Buxton, Derbyshire, SK17 9JN, 1988.
2. ZOHRABIAN, A.S., MOKHTARZADEH-DEHGHAN, M.R., REYNOLDS, A.J. MARRIOTT, B.S.T.
"An experimental study of buoyancy-driven flow in a half; scale stairwell model".
Building Environment, Vol. 24, No.2, pp. 141-148, 1989.
3. MÜNCH, W., RÜDEN, H., SCHKALLE, Y.D. and THIELE, F.
"Flow of micro-organisms in a hospital stair shaft - Full scale measurements and mathematical model".
Energy and Buildings, 9, pp. 253-262, 1986.
4. BROWN, W.G. and SOLVASON, K.R.
"Natural convection through rectangular openings in partitions - Vertical Partitions".
Int. J. Heat Mass Transfer, Vol.5, pp. 859-868, 1962.
5. SHAW, B.H.
"Heat and mass transfer by natural convection and combined natural and forced air flow through large rectangular openings in a vertical partition".
Instn. Mech. Eng., Cl17/71, pp.31-39, 1971.
6. SHAW, B.H. and WHYTE, W.
"Air movement through doorways - the influence of temperature and its control by forced airflow".
BSE. Dec. 1974, Vol. 42, pp. 210-218, 1974.
7. FEUSTEL, H., ZUERCHER, C.H., DIAMOND, R., DICKINSON, B., GRIMSRUD, D., and LIPSCHUTZ, R.
"Temperature and wind-induced air flow patterns in a staircase: Computer modelling and experimental verification".
Energy and Buildings, 8, pp. 105-122, 1985.
8. MARSHALL, N.R.
"The behaviour of hot gases flowing within a staircase".
Fire Safety Journal, 9, pp. 245-255, 1985.

9. MARSHALL, N.R.
"Air entrainment into smoke and hot gases in open shafts".
Fire Safety Journal, 10, pp. 37-46, 1986.
10. MAHAJAN, BAL M.
"Measurement of interzonal heat and mass transfer by natural convection".
Solar Energy, Vol. 38, No.6, pp 437-446, 1987.
11. RIFFAT, S.B., WALKER, J. and LITTLER, J.
"Zone to zone tracer gas measurement: Laboratory calibration and values of air flows up and down stairs in houses".
9th AIVC Conference "EFFECTIVE VENTILATION" 12-15 September 1988. Novotel, Gent., Belgium.
12. RIFFAT, S.B. and EID, M.
"Measurement of air flow between the floors of houses using a portable SF6 system".
Energy and Buildings, 12, pp. 67-75, 1988.
13. REYNOLDS, A.J.
"The scaling of flows of energy and mass through stairwells".
Build. and Envir., Vol. 21, Part 3/4, pp. 149-153, 1986.
14. REYNOLDS, A.J., MOKHTARZADEH-DEHGHAN, M.R. and ZOHRABIAN, A.S.
"The modelling of stairwell flows".
Build. and Envir., Vol. 23, No.1, pp. 63-66, 1988.
15. NEVRALA, D.J. and PROBERT, S.D.
"Modelling of air movement in rooms".
Journal of Mech. Eng. Science, Vol. 19, No.6, 1977.
16. LIDDAMENT, M.W.
"Modelling the influence of ventilation strategies on distribution and heat loss in a single family dwelling".
Proceedings of 2nd Int. Congress on Building Energy Management. 30 May - 3 June 1983, Iowa, USA.
17. ZOHRABIAN, A.S., MOKHTARZADEH-DEHGHAN, M.R., REYNOLDS, A.J.
"A numerical study of buoyancy-driven flows of mass and energy in a stairwell".
9th AIVC Conference "EFFECTIVE VENTILATION" 12-15 September 1988. Novotel, Gent., Belgium.
18. SIMCOX, S. and SCHOMBERG, M.
"Tunnel of Fire".
Science and Business. Nov-Dec Issue, 1988.

HEAT INPUT RATE \dot{Q} (W)	AIR CHANGE RATE \dot{Q}_S/V_S per hour	LEAKAGE RATE \dot{Q}_S (m ³ /s)	LEAKAGE RATE \dot{m}_L (kg/s)	EXTERNAL TEMP. T_R (°C)	EXTERNAL CONCENTRATION (PPM)
100	0.0659	5.42×10^{-5}	6.45×10^{-5}	19.5	150-160
300	0.0998	8.21×10^{-5}	9.69×10^{-5}	21.0	150-160
600	0.1085	8.92×10^{-5}	1.04×10^{-4}	21.5	180
900	0.1575	1.29×10^{-4}	1.49×10^{-4}	21.5	280

Table 1: Rate of leakage through the stairwell joints, for various heat input rates.

DISTANCE FROM SIDE WALL (m)	\dot{Q} (W)	U_{maxu} (m/s)	U_{maxd} (m/s)	T_H (°C)	T_C (°C)
w/2	100	0.17	0.24	29.7	28.3
	300	0.28	0.31	35.4	32.1
	600	0.36	0.36	43.6	36.8
	900	0.42	0.54	50.1	41.8
5w/12	100	0.16	0.23	29.8	28.0
	300	0.27	0.27	35.5	31.6
	600	0.34	0.36	43.6	37.3
	900	0.41	0.54	50.4	41.5
w/3	100	0.17	0.22	29.7	27.8
	300	0.27	0.27	35.5	31.6
	600	0.34	0.36	43.4	37.2
	900	0.46	0.50	50.7	41.1
w/4	100	0.17	0.21	29.8	27.3
	300	0.26	0.23	35.5	31.1
	600	0.32	0.32	43.2	37.0
	900	0.38	0.47	50.6	42.5
w/6	100	0.17	0.18	28.0	26.8
	300	0.24	0.21	35.0	30.2
	600	0.31	0.31	42.5	36.2
	900	0.35	0.47	49.6	41.4
w/12	100	0.17	0.16	27.6	26.0
	300	0.24	0.18	32.8	28.2
	600	0.31	0.31	39.9	34.7
	900	0.31	0.47	46.3	37.7

Table 2: Maximum velocities and mean temperatures in the upflow and downflow streams (at the throat area) at w/2, 5w/12, w/3, w/4, w/6, w/12 for various heat input rates.

\dot{Q} (W)	\dot{V}_u (m ³ /s)	\dot{V}_d (m ³ /s)	\dot{V}_m (dm ³ /s)	\dot{m}_u (kg/s)	$(\dot{m}_d + \dot{m}_l)$ (kg/s)
100	0.0223	0.0220	22.15	0.0251	0.0245
300	0.0297	0.0288	29.25	0.0327	0.0322
600	0.0378	0.0382	38.00	0.0410	0.0415
900	0.0490	0.0512	50.10	0.0515	0.0543

Table 3: Volume and mass flow rates in the upflow and downflow (including leakage), at throat area for various heat input rates.

CORRESPONDING WALL	100 (W)	300 (W)	600 (W)	900 (W)
AC	15.6	39.9	67.4	95.6
CD	4.7	17.2	41.5	45.5
DE	3.0	7.3	18.2	23.1
EF	6.3	29.4	58.7	83.0
FG	3.7	9.6	18.1	26.7
GH	2.5	6.1	12.1	18.7
HI+IA	5.5	16.8	33.5	42.8
SIDE WALLS	58.6	164.0	350.4	583.9
LEAKAGE	0.6	1.1	1.8	3.1
TOTAL LOSS	100.5	291.4	601.7	922.4

Table 4: Rate of heat loss from the stairwell at various heat input rates (see Figure 1).

CORRESPONDING WALL	300 W	600 W
AC	46.2	85.0
CD	33.6	66.2
DE	15.2	38.9
EF	76.6	178.7
FG	21.3	42.2
GH	14.1	38.4
HI	42.8	67.1
IA	37.0	67.5
LEAKAGE	1.6	2.5
TOTAL LOSS	288.4	586.5

Table 5: Rate of heat loss from the stairwell, with insulated side walls (see Figure 1).

\dot{Q} (W)	T_{av} (°C)	\dot{V}_m (dm ³ /s)	1000xFr	1000xSt	Re	Gr	DT (Cdeg)
100	28.1	22.15	13.85	0.1765	2060	9.733x10 ⁷	1.7
300	31.8	29.25	18.33	0.5287	2650	2.179x10 ⁸	4.1
600	38.9	38.00	23.81	1.0567	3300	2.945x10 ⁸	6.1
900	41.9	50.10	31.31	1.5845	4400	3.819x10 ⁸	8.6

Table 6: Basic performance characteristics of the closed-stairwell geometry.

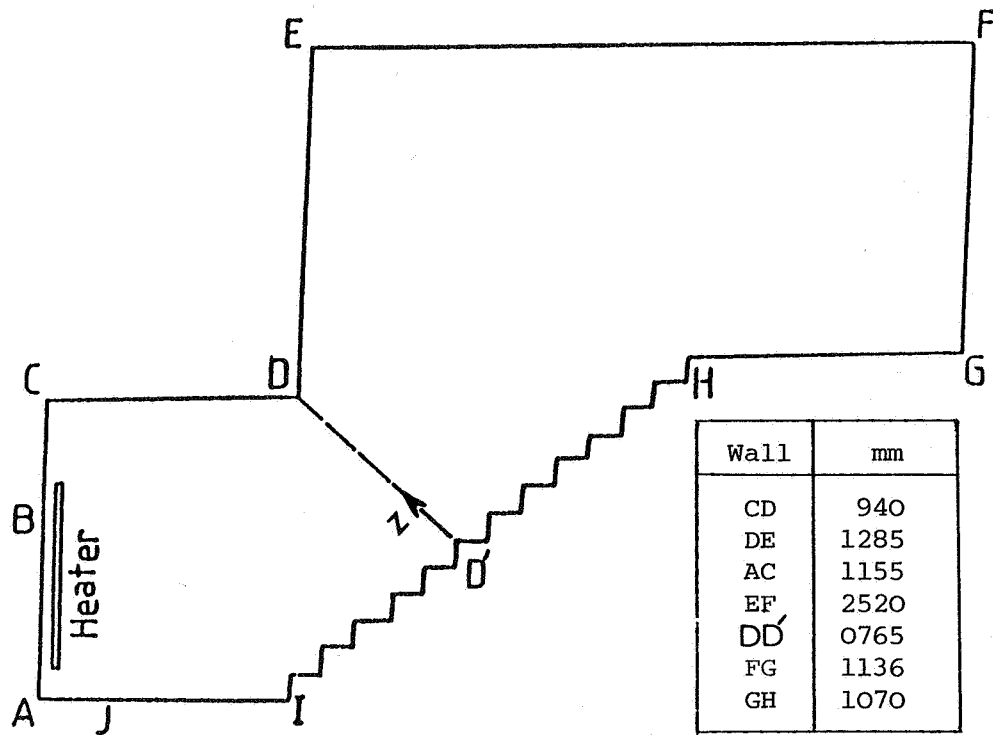


Figure 1. Schematic diagram of the half-scale stairwell model.

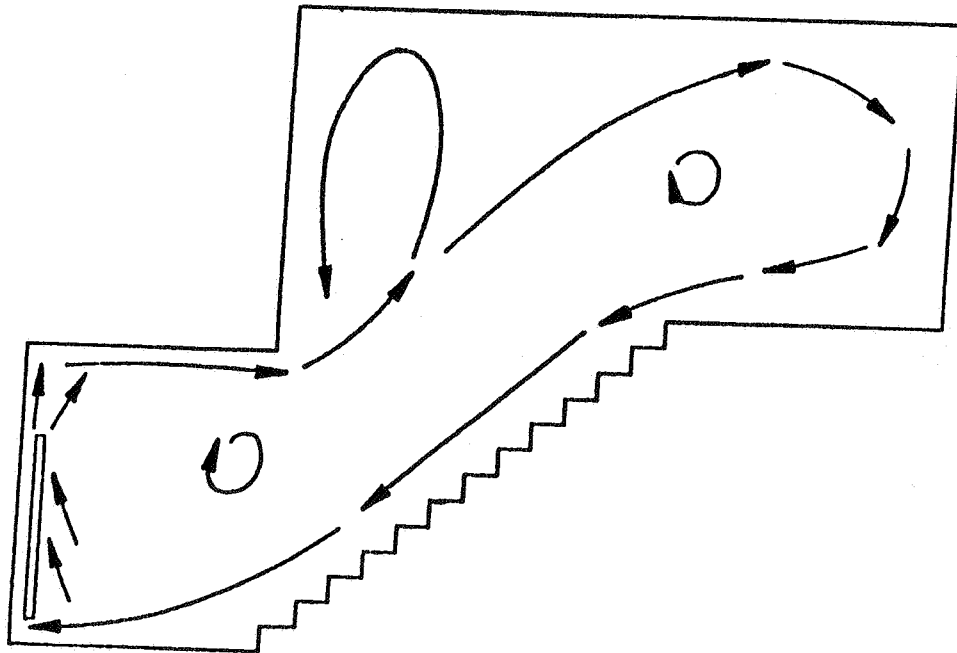


Figure 2. A two-dimensional view of the flow pattern in the stairwell.

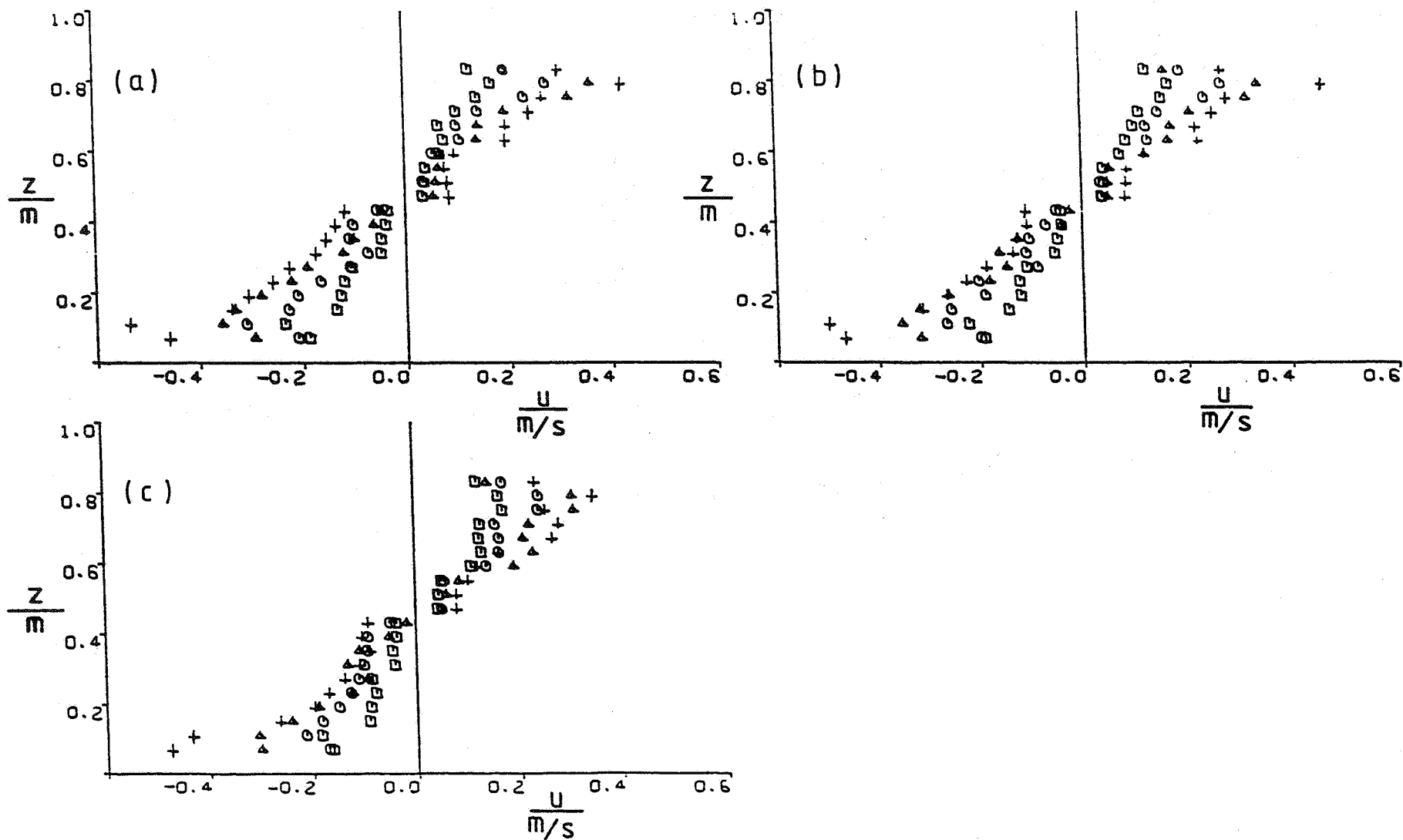


Figure 3

Velocity profiles at various distances from the side wall for various heat input rates.

(a) $w/2$, (b) w/s , (c) $w/6$

□ 100 W, ○ 300 W, △ 600 W, + 900 W.

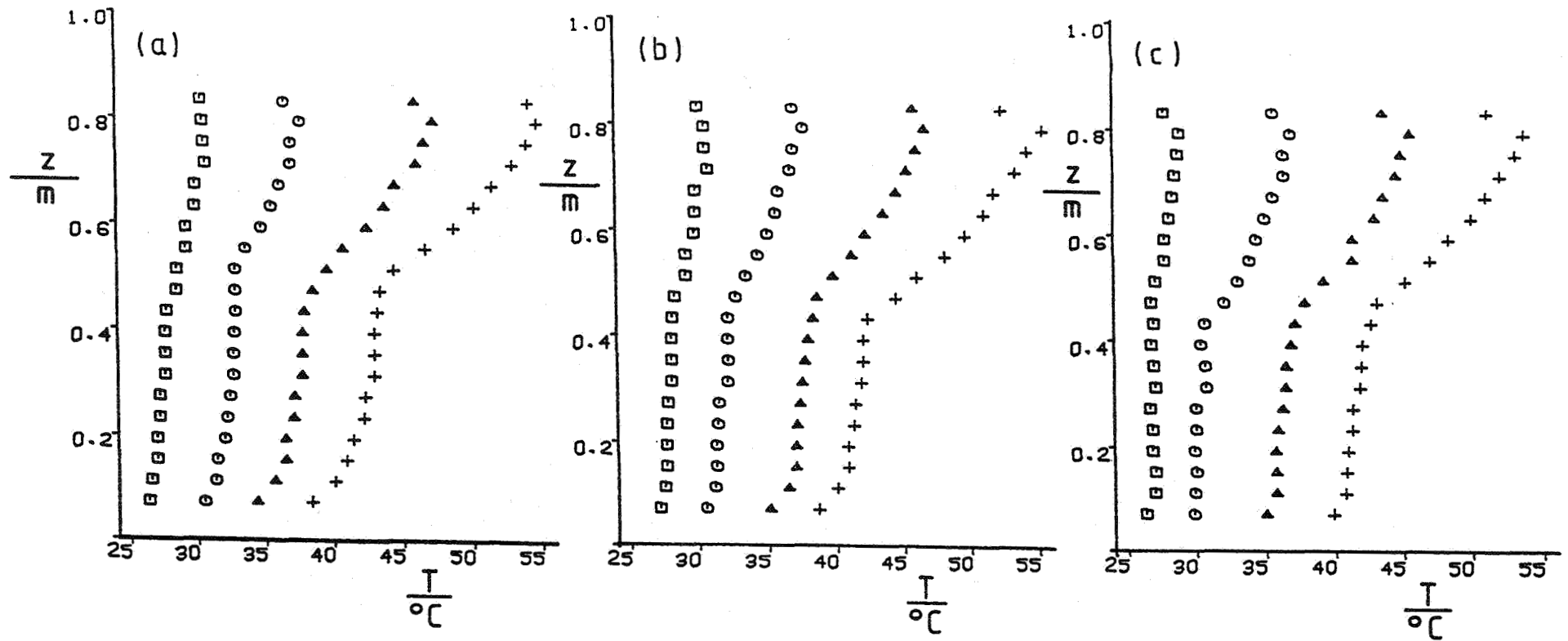


Figure 4

Temperature distributions at various distances from the side wall, for various heat input rates.

(a) $w/2$, (b) $w/3$, (c) $w/6$

□ 100 W, ○ 300 W, △ 600 W, + 900 W.

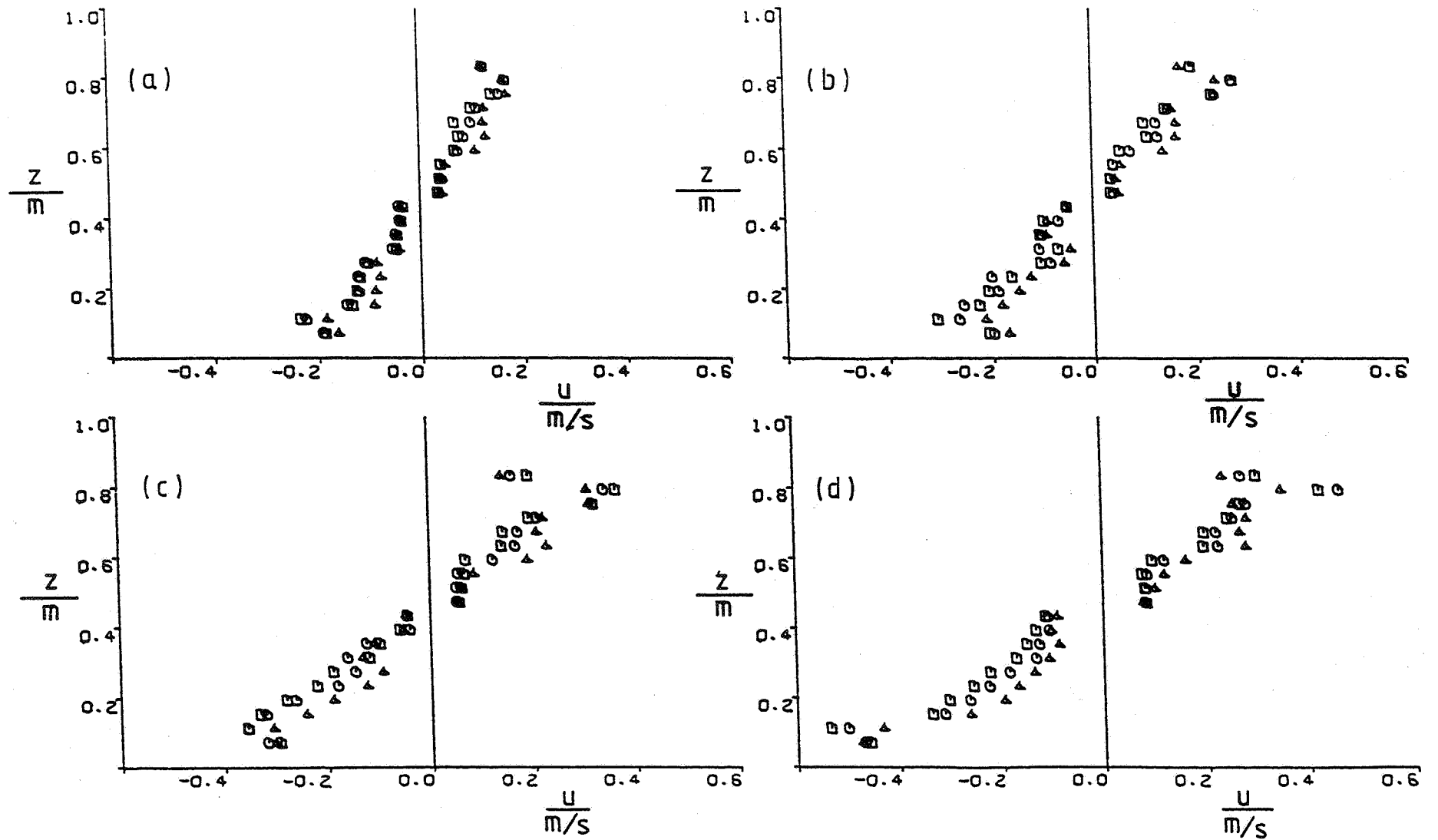


Figure 5. Velocity profiles for various heat input rates, at various distances from the side wall.
 (a) 100 W, (b) 300 W, (c) 600 W, (d) 900 W.
 O $w/2$, □ $w/3$, Δ $w/6$.

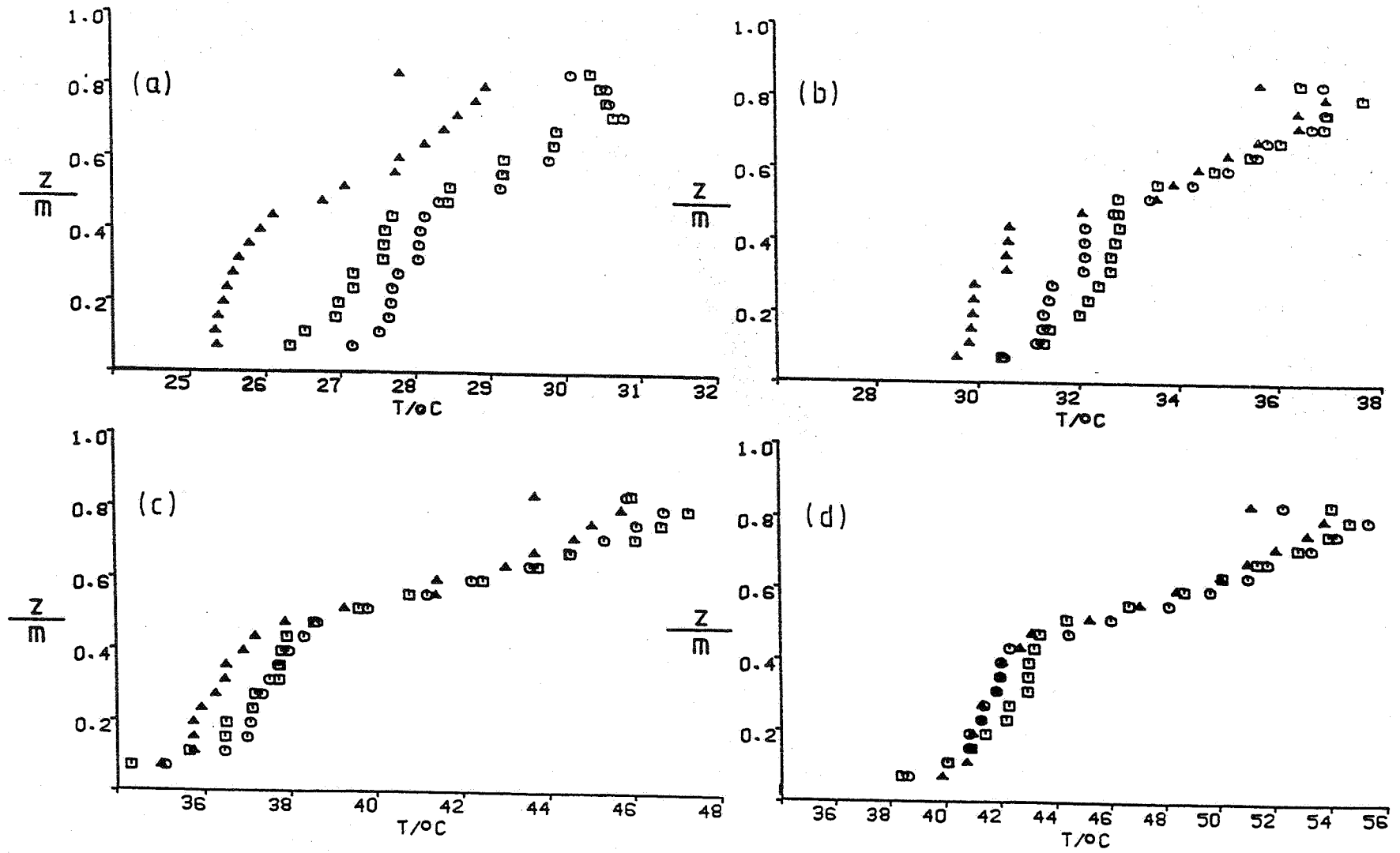


Figure 6 Temperature distributions for various heat input rates, at various distances from the side wall. (a) 100 W, (b) 300 W, (c) 600 W, (d) 900 W. \circ $w/2$, \square $w/3$, Δ $w/6$.

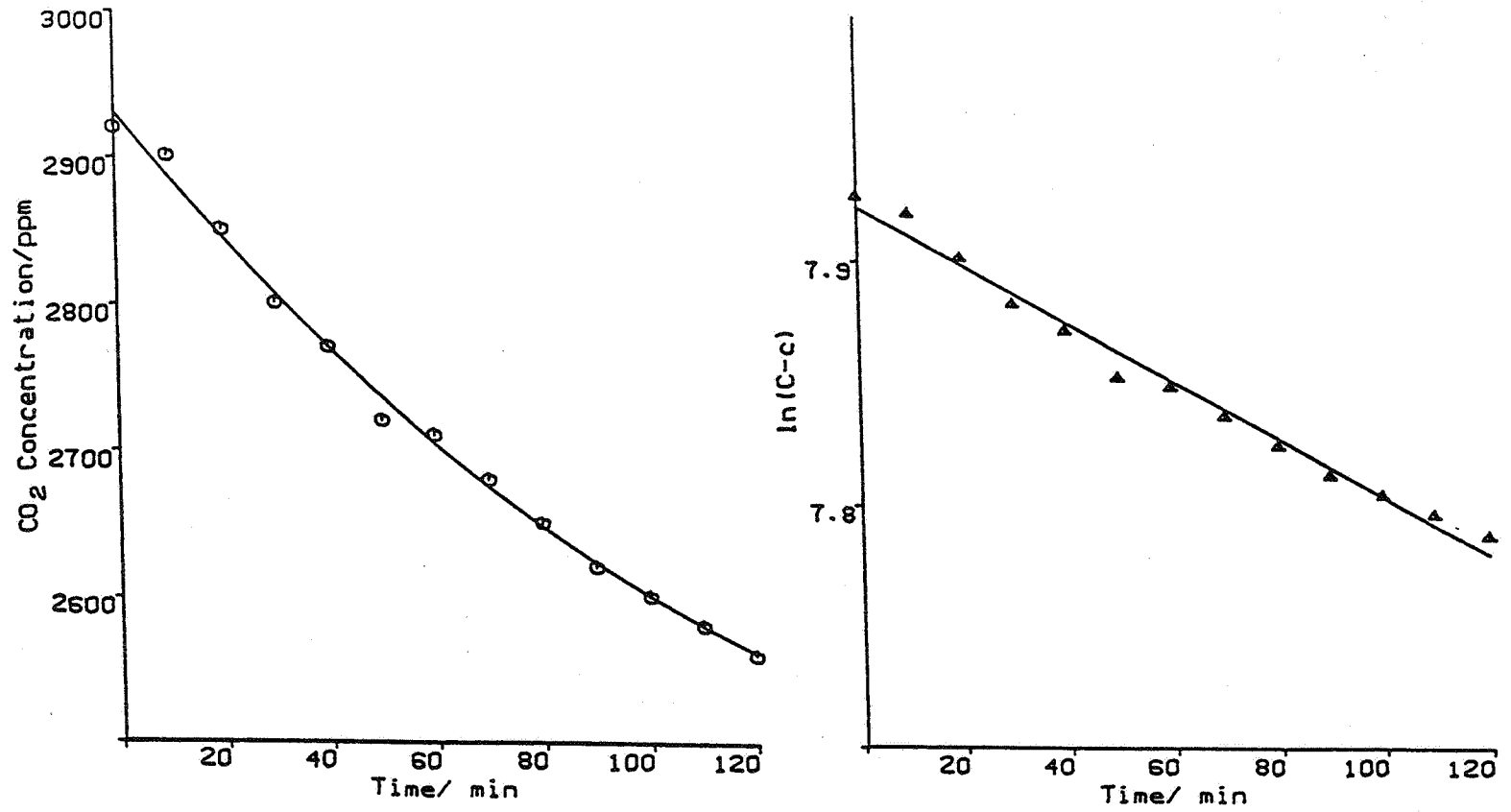


Figure 7. Typical curve of the CO₂ tracer gas concentration against time.
(Heat input rate = 100 W).